ISSN 1855-9913

Journal of the Laser and Health Academy
Vol. 2014, No.1; www.laserandhealth.com

Dependence of Skin Ablation Depths on Er:YAG Laser Fluence

Karolj Nemes[1], Janez Diaci[2], Uros Ahcan[3], Leonardo Marini[4], Matjaz Lukac[1]

[1]Fotona, Ljubljana, Slovenia
[2]University of Ljubljana, Faculty of Mechanical Engineering, Ljubljana, Slovenia
[3]University Clinical Center Ljubljana, Department of Plastic Surgery and Burns, Ljubljana, Slovenia
[4]Skin Doctors Clinic, Trieste, Italy

ABSTRACT

Triangulation and histological studies were made of skin ablation depths following skin treatments with a Fotona Dynamis Er:YAG laser system. The following laser handpieces were used in the study: Full beam handpieces R04 and R11; Stamping patterned handpieces PS01, PS02 and PS03; fractionated handpiece FS01 and c) Scanning fractional handpiece F22.

The laser fluence (F) was found to be the major parameter that determines the ablation depth during Er:YAG skin treatments. Here, F=E/A, where ***E*** is the energy of the laser pulse, and A is the laser spot size area. Above the ablation threshold F_{thr}, the ablation depth (D) was found to grow approximately linearly with the fluence as $D = K \times (F - F_{thr})$ where $K \approx 4$ μm.cm²/J. For the same fluence, ablation depths were within experimental error independent of pulse duration, pulse energy and spot size.

With identical fluences, the ablation depths achieved with the full beam handpieces R04 and R11 were measured to be the same as those obtained with the patterned beam handpieces PS01, PS02 and PS03, and as well with the stamping fractionated handpiece FS01. This is due to the fact that the Fotona Dynamis patterned and stamping fractionated handpieces do not use any focusing optics to create smaller micro beams. Instead, the full beam is divided into smaller beams by a metal screen or diffractive optics. As a result, the fluence of each individual micro beam remains unchanged and is of the same top-hat spatial distribution of the full beam.

Ablation depths achieved with the scanning fractional handpiece F22 were found to follow the same linear dependence on laser fluence.

Key words: Er:YAG laser; ablation depth; full beam handpiece, stamping patterned handpiece, fractionated handpiece

Article: J. LA&HA, Vol. 2014, No.1; pp.07-13.
Received: December 12, 2013; Accepted: February 24, 2014

I. INTRODUCTION

In the last decade, cutaneous laser resurfacing using the Er:YAG laser has gained popularity among laser surgeons and the public [1-10]. Among all laser wavelengths, the cutaneous absorption of the Er:YAG laser energy by water is the highest, allowing for superficial tissue ablation and fine control.

Appropriate laser parameters depend on the type of Er:YAG laser system used and the specific resurfacing indication. In this study, we carried out in-vivo histological and ex-vivo triangulation measurements in order to develop a systematic understanding of the ablative effects of the Fotona Dynamis Er:YAG laser handpieces.

II. MATERIALS AND METHODS

a) Laser and handpieces

The Er:YAG laser used in the study was a **Fotona Dynamis Er:YAG laser system** (Fig. 1)

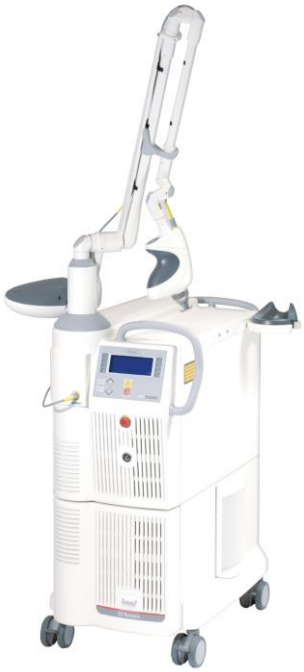

Fig. 1: Fotona Dynamis Er:YAG laser system.

The Dynamis laser system was fitted with one of the following handpieces:

a) **R04** and **R11** full beam handpieces,

b) **PS01**, **PS02** and **PS03** patterned handpieces

c) **FS01** stamping fractionated handpiece

d) **F22** scanning fractionated handpiece.

There are two approaches to skin resurfacing: full-field (or full beam) and fractional [30-38]. In full-field resurfacing, the entire surface area of the skin within the laser spot is affected by the laser. The fractional technique is based on a concept of producing an array of microscopic wounds on the skin surface that are rapidly re-epithelialized by the surrounding, undamaged tissue, sparing the epidermis in the untreated areas (Fig. 2).

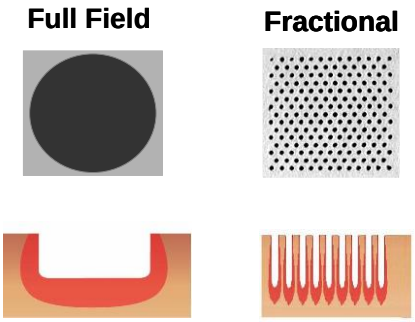

Fig. 2: As opposed to full-field resurfacing, fractional resurfacing is based on a concept of producing an array of smaller wounds.

There are also two types of fractionated handpiece technologies, stamping and scanning (Fig. 3).

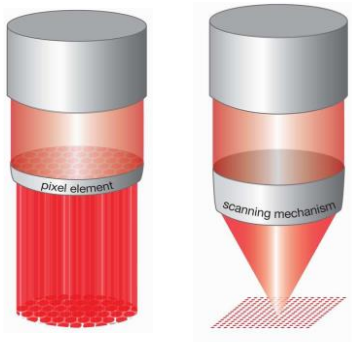

Fig. 3: Two types of fractionated handpiece technologies.

With stamping handpieces, the full laser beam (spot) is divided into many small beams (micro beams or pixels), and the pixel fluence is comparable to the total laser beam fluence. The pixel energy is a fractional part of the total pulse energy.

With scanning fractionated handpieces, the laser beam is concentrated and focused into a very small micro beam that is scanned over a treated area. The micro beam energy is the same as the full-field pulse energy which enables higher fluences and deeper treatments. Also, the treatment areas and the pixel density can be easily changed via the keyboard.

The Fotona Er:YAG Dynamis laser system allows the practitioner to use the following manual handpieces: three patterned titanium handpieces: **PS01**, **PS02** and **PS03,** and fractionated handpiece **FS01** in addition to two full beam titanium handpieces **R04** and **R11** (see Fig. 4).

	R04 full beam handpiece.
	R11 full beam handpiece.
	The PS01 patterned handpiece consists of a full beam R04 handpiece with an installed metal screen at the output part of the handpiece.
	The PS02 patterned handpiece consists of a full beam R04 handpiece with an installed metal screen inside the handpiece optics.
	The PS03 patterned handpiece consists of a full beam R11 handpiece with an installed metal screen inside the handpiece optics.
	The FS02 fractionated handpiece consists of a full beam R04 with an installed an additional diffractive optical element in front of the same focusing lens, and there is a single detachable spacer that defines the position of the focal plane of exit lens.

Fig. 4: Fotona Dynamis Er:YAG laser manual handpieces. Patterned and fractionated handpieces are identical to full beam handpieces in their construction, the only difference is an additional metal screen or diffractive optical element installed.

The Fotona Dynamis manual handpieces PS01, PS02, PS03 and FS01 **do not use any focusing optics** to create smaller micro beam dots. Instead, the full beam is divided into smaller beams.

As a result, **the fluence of each individual micro beam remains unchanged and is the same to that of the full beam**. Here, the fluence (F) is defined as energy density, $F = E/A$ (in J/cm^2), where E is the

energy of the laser pulse, $A = \pi s^2/4$ is the micro beam spot size area, and s is the spot size diameter of the laser beam at the skin surface.

The Fotona scanning fractionated handpiece F22 (F-Runner) is shown in Fig. 5. The F-Runner utilizes a fixed, 250 μm spot size and offers a 2% to 60% coverage range. As opposed to the manual stamping handpieces, **the full beam of the scanning F22 fractionated handpiece is focused into a single small spot of 250 microns diameter, and thus much higher fluences and ablative depths can be achieved**.

Fig. 5: Scanning fractionated handpiece F22 (F-Runner, Fotona d.d.).

b) Laser triangulation measurements

Human skin obtained during abdominal surgery was used in the study. Because of the very small volumes of ablated skin in many of the measurements, a highly-accurate methodology was required to make the appropriate measurements of the ablated depths in the skin.

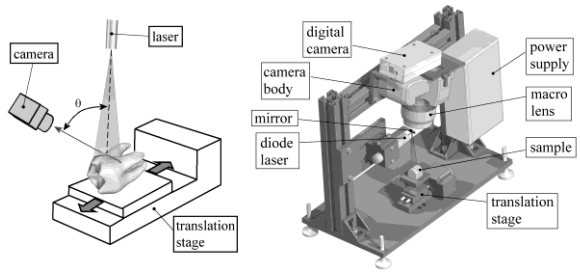

Fig. 6: Schematic showing operation of profilometer, and general assembly of the equipment.

To achieve this, a specialized measurement assembly has been developed and proven to be effective at the Faculty of Mechanical Engineering at the University of Ljubljana, Slovenia. This makes use of a laser profilometer running in conjunction with custom 'Volume_analyser' software [12-14]. The method is based on the optical triangulation principle. The measured surface is illuminated by a diode laser beam, formed into a light plane. The bright laser beam is visible on the illuminated surface and captured by a camera (See Fig. 6). The design of the system ensures highly-accurate and repeatable measurements as well as the facility for photographic recording and visual comparisons (see Fig. 7).

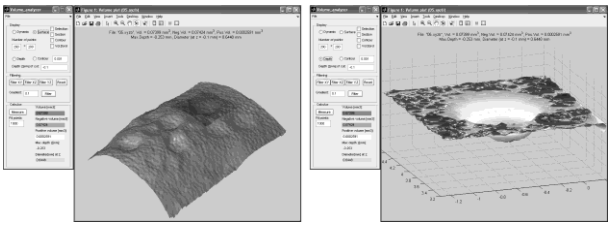

Fig. 7: Screenshots of 'Volume_analyser' software showing various stages in volume analysis.

Typical examples of the triangulation images of Er:YAG laser ablated holes are shown in Fig. 8.

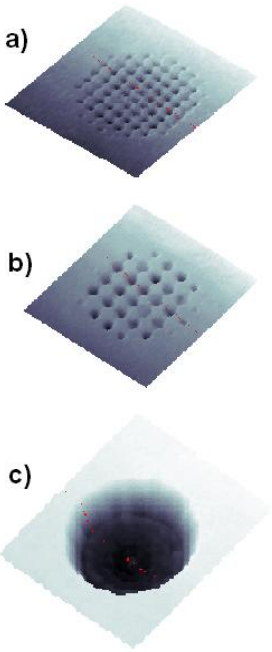

Fig. 8: Triangulation images of the ablated holes following a treatment with: a) stamping patterned handpiece PS01, position 1.7mm overall spot size; b) stamping patterned handpiece PS01, position 3.7mm overall spot size; c) full beam handpiece R04, 7 mm spot size.

c) Histological measurements

The histological data of six male patients were analyzed. All patients consented to biopsies following the treatment with the Dynamis Er:YAG F22 scanning fractionated handpiece.

d) Theoretical calculations

Most researchers agree that the erbium lasers' high ablation efficiency results from micro-explosions of overheated tissue water [11, 15]. This type of thermo-

mechanical ablation mechanism must be distinguished from mechanisms involving strong acoustic transients, plasma formation, or transient bubble formation, which can be encountered at higher laser intensities. Here, we apply a previously developed microscopic physical model of the micro-explosions [28]. The previously published model examined only the initiation of explosive material removal. In this paper, we improve upon this model by considering the ablation process above the ablation threshold. In the model, the process of confined boiling is modeled by considering the thermodynamic behavior of tissue water when it is heated within an elastic tissue [28]. The thermodynamic behavior of tissue water, which is the major absorber of Er:YAG (2.94 mm) laser irradiation, is combined with the elastic response of the surrounding solid medium. This is complemented by one-dimensional treatment of heat diffusion using a finite-difference scheme, and modeling protein denaturation kinetics with the Arrhenius integral [34]. The developed model explicitly links laser and tissue parameters with the end effects of ablation and residual heat deposition. We used this model to determine the influence of laser parameters on the desired surgical end effects in the treated tissue.

III. RESULTS

a) In-vitro Ablation Depth Measurements

The fluence (F) is one of the main settings for skin resurfacing. It is defined as energy density:

$$F = E/A \qquad (1)$$

Where E is the energy of the laser pulse, $A = \pi s^2/4$ is the spot size area, and s is the spot size diameter of the laser beam at the skin surface. Usually it is calculated in J/cm². Typical Er:YAG fluences for a skin resurfacing are between 0.5 to 50 J/cm².

Figure 9 shows the ablation depths, as calculated using the MEC micro-explosions computer model, for different pulse durations as a function of laser fluence.

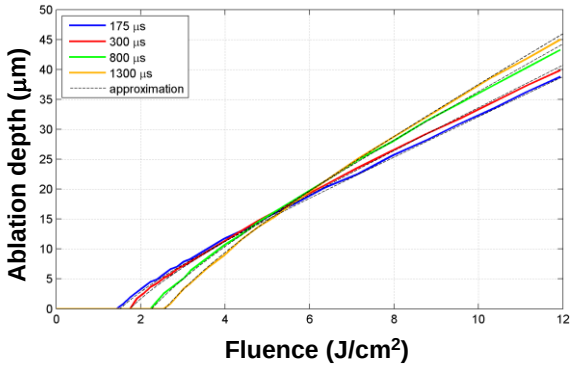

Fig. 9: Dependence of skin ablation depth on laser pulse fluence and pulse duration, as calculated from the MEC micro-explosions computer model.

The above calculated results are highly congruent with the in-vitro measurements of ablation depths in human skin obtained during abdominal surgery. Figure 10 shows ablative depths as measured with the laser triangulation technique for the full beam handpiece R04 set to a 3 mm spot size.

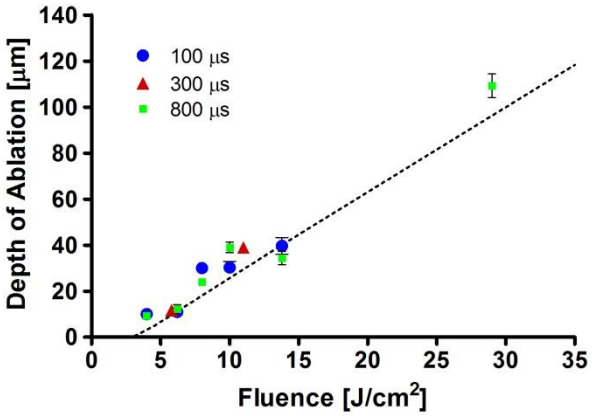

Fig. 10: Dependence of human skin ablation depth on laser pulse fluence and pulse duration, as measured with the laser triangulation method (R04 handpiece, 3 mm spot size). The ablation depth (D) depends linearly on the pulse fluence (F) as D= K x F where K = (3.7+- 0.3) µm cm²/J.

The MEC model and the experiment show that there is a threshold fluence under which there is no ablation (non-ablative regime). Ablation threshold fluence depends slightly on the pulse duration (it is higher for longer pulse durations), and ranges from 1.6 to 2.2 J/cm². Note that clinically a slight ablation may be observed already at lower fluences. This is attributed to skin surface in homogeneities and surface sweat that facilitate earlier ablation.

Figure 11 shows that above the ablation threshold F_{thr}, the measured ablation depth (D) grows approximately linearly with the fluence as D = K x (F - F_{thr}) where K = 3.7 µm cm²/J. Note that the dependence of the ablation depth on the pulse duration is relatively weak. The major parameter is the laser pulse fluence. Note also that the exact values of the ablation threshold and of the linear ablation slope (K) will depend on the patient skin type, treatment location, skin hydration level and other conditions.

The laser pulse energy is a good predictor of the ablative depth only when the same spot size is used. For the same fluence at different spot sizes, the pulse laser energy will vary considerably, while the ablative depth will be the same. Figure 11 shows that for different spot sizes, the ablative effect will be the same for the same fluence but not for the same pulse energy. For example, at a fluence of 5J/cm², an ablative depth of approximately 10 µm will be achieved with a pulse energy of: 350 mJ with a 3 mm spot size, 980 mJ with a 5

mm spot size, and 1920 mJ with a 7 mm spot size.

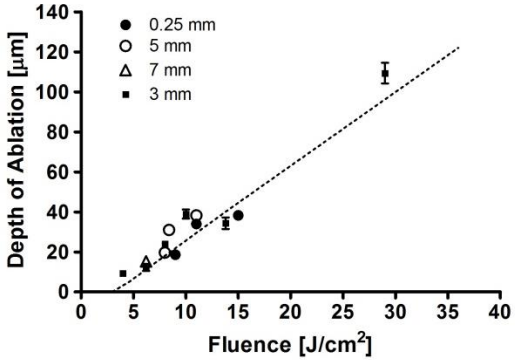

Fig. 11: Dependence of ablation depth on laser pulse fluence and spot size, as measured with the laser triangulation method using full beam R04 handpiece and fractionated FS01 handpiece, 300 µs pulse duration). The ablation depth (D) depends linearly on the pulse fluence (F) as D= K x F where K = (3.8+- 0.3) µm cm²/J.

The Fotona Dynamis manual stamping handpieces PS01, PS01, PS03 and FS01 do not use any focusing optics to create smaller beam dots. Instead, the full beam is divided into smaller beams by a metal screen or diffractive optical element. As a result, the fluence of each individual fractionated beam remains unchanged and is the same as that of the full beam. Here, the fluence (F) is defined as energy density, $F = E/A$ (in J/cm²), where E is the energy of the laser pulse, $A = \pi s^2/4$ is the micro beam spot size area, and s is the spot size diameter of the laser beam at the skin surface. The ablative effect of the stamping handpieces PS01, PS02, PS03 and FS01 on the human skin is thus identical to the ablative effect of the full beam handpieces R04 or R11. Figure 12 shows the ablation depths for different types of handpieces. The ablative depths follow the same linear dependence on laser fluence, independently of the handpiece type.

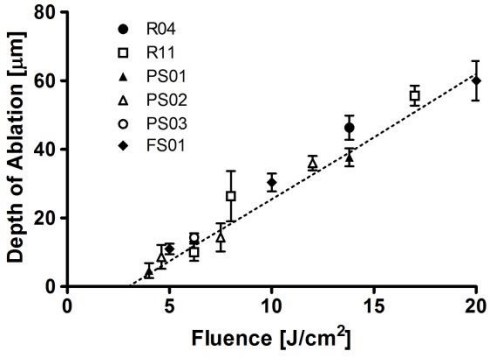

Fig. 12: Dependence of ablation depth on laser pulse fluence and handpiece type, as measured with the laser triangulation method). The ablative depths follow the same linear dependence of laser full beam or micro beam fluence, independently of the handpiece type. The ablation depth (D) depends linearly on the pulse fluence (F) as D= K x (F- F_{thr}) where K = (3.7+- 0.4) µm cm²/J.

Since the triangulation method is not suitable for measuring very deep holes, the ablative effect of the scanning fractionated handpiece F22 was measured by obtaining histological results following the Er:YAG laser treatments. A typical histological picture of a hole in the human skin following treatment with the F22 handpiece is shown in Fig. 13.

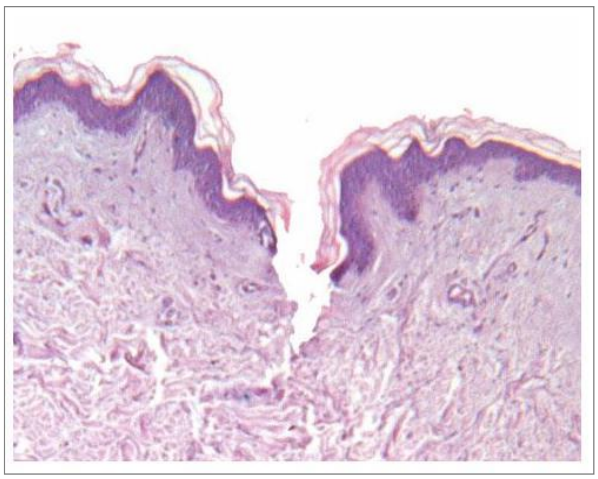

Fig. 13: A histological picture of an ablated pixel, using the scanning fractionated handpiece F22 (laser energy 30 mJ).

The dependence of the ablation depth on the F22 handpiece pulse energy as obtained from histological pictures is shown in Fig. 14. The Er:YAG pulse duration was 300 µs.

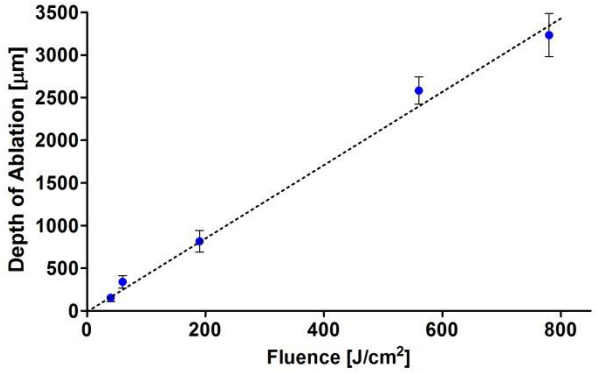

Fig. 14: Dependence of ablation depth on micro beam fluence for the F22 scanning fractionated handpiece, as obtained from histological results. The ablation depth (D) depends linearly on the maximal pulse fluence within a micro beam as D= K x (F- F_{thr}) where K = (4.3+- 0.2) µm cm²/J.

IV. DISCUSSION

The optical technologies in the two fractionated handpieces, F22 and FS01 are different. The micro beam of the F22 handpiece is generated by focusing an apertured full beam into a single intense micro beam that is being scanned over a treatment area. On

the other hand, the micro beams of the FS01 handpiece are generated by diffracting (using a diffraction lens) the full beam into a large number of simultaneous micro beams. The spatial beam distribution of the micro beams is therefore slightly different for the two fractionated handpieces. The micro beam spatial distribution of the FS01 handpiece is with approximately a top-hat beam profile while the spatial distribution of the F22 micro beam follows approximately the shape of an Airy function. In order to compare the ablation efficacy of both types of handpieces, the nominal diameter of the F22 micro beam was defined to represent the diameter at one third of the beam's maximal amplitude. Using this definition, the peak amplitude is approximately the same for the micro beams of both types of fractionated handpieces, providing the micro beam energies and nominal beam diameters are the same. This was confirmed experimentally where approximately the same ablation factor K was obtained for both types of fractionated handpieces.

V. .CONCLUSIONS

Dependences of human skin ablation on Er:YAG laser parameters were determined for different pulse durations, spot sizes and handpieces. The laser fluence F = E/A, where E is the pulse energy and A is the laser spot area, was found to be the most important parameter for determining the ablation depth. For all pulse durations, spot sizes and laser handpieces, the ablation depth (D) was determined to depend approximately linearly on the laser fluence: $D = K \times (F - F_{thr})$ where K was approximately equal to 4 □ m cm^2/J.

ACKNOWLEDGMENT

This research was carried out in a collaboration with the EU regional Competency Center for Biomedical Engineering (www.bmecenter.com), coordinated by Laser and Health Academy (www. laserandhealthacademy.com), and partially supported by the European Regional Development Fund and Slovenian government.

REFERENCES

1. T.C. Spoor, R.L. Moy, Facial Rejuvenation, Martin Dunitz Ltd. 2001, pp. 105-148.
2. Utley DS, Koch RJ, Egbert BM. Histologic analysis of the thermal effect on epidermal and dermal structures following treatment with the superpulsed CO2 laser and the erbium: YAG laser: an in vivo study. *Lasers Surg Med.* 1999;24(2):93-102.
3. Tanzi EL, Alster TS. Single-pass carbon dioxide versus multiple-pass Er:YAG laser skin resurfacing: a comparison of postoperative wound healing and side-effect rates. *Dermatol Surg.* Jan 2003;29(1):80-4.
4. Cole RP, Widdowson D, Moore JC. Outcome of erbium:yttrium aluminium garnet laser resurfacing treatments. *Lasers Med Sci.* Oct 2008;23(4):427-33.
5. K. Kunzi-Rapp, C.D. Dierickx, B. Cambier, M. Drosner, Minimally invasive skin rejuvenation with erbium: YAG laser used in thermal mode, Lasers in Surg. and Med. 38, pp 899-907, 2006.
6. Pozner JN, Roberts TL 3rd. Variable-pulse width ER:YAG laser resurfacing. *Clin Plast Surg.* Apr 2000;27(2):263-71.
7. Alster TS, Lupton JR. Erbium:YAG cutaneous laser resurfacing. *Dermatol Clin.* Jul 2001;19(3):453-66.
8. Teikemeier G, Goldberg DJ. Skin resurfacing with the erbium:YAG laser. *Dermatol Surg.* Aug 1997;23(8):685-7.
9. Pozner JN, Goldberg DJ. Superficial erbium:YAG laser resurfacing of photodamaged skin. *J Cosmet Laser Ther.* Jun 2006;8(2):89-91.
10. Kaufmann R. Role of Erbium:YAG laser in the treatment of aged skin. *Clin Exp Dermatol.* Oct 2001;26(7):631-6.
11. B. Majaron, P. Plestenjak, M. Lukac, Thermo-mechanical laser ablation of soft tissue: modeling the micro-explosions, Appl.Phys.B 69,71-80 (1999).
12. T. Perhavec, J. Diaci. Comparison of Er :YAG and Er,Cr :YSGG dental lasers, J. Oral Laser Appl., 2008 ;8 :87-94.
13. T. Perhavec, A. Gorkič, D. Bračun, J. Diaci. A method for rapid measurement of laser ablation rate of hard dental tissue, Optics and Laser Technology, 2009; 41(4). 397-402.
14. J. Diaci, Laser Profilometry for the Characterization of Craters Produced in Hard Dental Tissues by Er:YAG and Er,Cr:YSGG Lasers, J. Laser and Health Academy, 2008/2.
15. A. Vogel, V. Vengugopalan, Mechanisms of Pulsed Laser Ablation of Biological Tissues, Chem. Rev. 2003,103, 577-644.
16. B. Majaron, D. Sustersic, M. Lukac, U.Skaleric, N. Funduk, Heat diffusion and debris screening in Er:YAG laser ablation of hard biological tissues, Appl.Phys.B, 66, 1-9 (1998).
17. Beltram M., B. Drnovsek-Olup. New collagen synthesis in skin fibroblasts after Er:YAG laser skin resurfacing. *Lasers surg. med.*, March 2005, suppl. 17, pp. 33.
18. M. Beltram , B. Drnovsek-Olup. Quantitative analysis of new collagen synthesis after Er:YAG laser skin resurfacing with biomolecular technique. *Lasers surg. med.*, 2008, suppl. 20, pp. 35.
19. B. Drnovsek-Olup, M. Beltram . ER:YAG dual-mode skin resurfacing long-term follow-up. *Lasers surg. med. (Online)*, Oct. 2002, pp. 1-9.
20. M. Beltram , B. Drnovsek-Olup. In situ hybridization analysis of type 1 collagen gene expression after Er:YAG laser skin resurfacing. *Lasers surg. med., Suppl.*, 2003, suppl. 15, pp. 8.
21. B. Drnovsek-Olup, M. Beltram , J. Pizem. Repetitive Er:YAG laser irradiation of human skin : a histological evaluation. *Lasers surg. med.*, 2004, vol. 35, no. 2, pp. 146-151.
22. B. Drnovsek-Olup, M. Beltram . Long term evaluation of periocular Er:Yag laser skin resurfacing combined with blepharoplasty. V: ESOPRS Meeting. *Abstracts.* [Münster: Universitäte-Hauptgebäude, 2002].
23. B. Drnovsek-Olup, M. Beltram . Er:Yag laser skin resurfacing long term follow-up. *Lasers surg. med.*, 2002, suppl. 14, pp. 66-67.
24. B. Drnovsek-Olup, M. Beltram . Collagen synthesis after laser skin resurfacing : in situ hybridization of pro alpha 1 collagen type 1. V: *ESOPRS Gothenburg 2003: [abstracts].*
25. M. Beltram, B. Drnovsek-Olup. Histological and biomolecular analysis of new collagen synthesis after Er:YAG laser skin resurfacing. V: *Alpe Adria community ophthalmology 2004 : [program & abstracts book], October 8th to 10th, 2004*. Munich: University of Technology, 2004, pp. 73.
26. M. Beltram, B. Drnovsek-Olup. Histological and biomolecular analysis of new collagen synthesis after "smooth" mode Er:Yag laser skin. *Lasers surg. med.*, 2004, suppl. 16, pp. 56.
27. B. Drnovsek-Olup, M. Beltram. Histological comparison between different modes of Er:YAG laser skin resurfacing-ablative, dual mode and smooth mode resurfacing. *Lasers surg. med.*, March 2005, suppl. 17, pp. 9.
28. B. Drnovsek Olup, B. Vedlin, Use of Er:YAG laser for benign skin disorders, Lasers in Surg. and Med. 21, pp 13-19, 1997.

29. B. Majaron, S.M. Srinivas, H.L. Huang, J.S. Nelson, Deep thermal of dermal collagen with repetitive Er:YAG laser irradiation, Lasers in Surg. and Med. 26, pp 215-222, 2000.
30. C. C. Dierickx et al., Micro-Fractional Ablative Skin Resurfacing with Two Novel Erbium Laser Systems, Lasers in Surg. and Med. 40, pp 113-123, 2008.
31. Pozner JN, Glanz S, Goldberg DJ. Fractional erbium resurfacin: Histologic and early clinical experience, Lasers in Surg. and Med. 39, pp S19:73, 2007.
32. M. Lapidoth, M.E.Y. Odo, L.M. Odo, Novel Use of Erbium (2,940nm) Laser for Fractional Ablative Photothermolysis in the Treatment of Photodamaged Facial Skin: A Pilot Study, Dermatology Surgery, 2008:34:2-6.
33. L.Volovec: Skin Rejuvenation with Fractionated Ablative Er:YAG Laser, 7th Croatian Congress of Plastic, Reconstructive and Aesthetic Surgery, Book of abstracts, Split, Croatia 1-5 October, 2008.
34. M. A. Trelles, M. Velez, S. Mordon, Correlation of Histological Findings of Single Session Er:YAG Skin Fractional Resurfacing With Various Passes and Energies and the Possible Clinical Implications, Lasers in Surg. and Med. 40, pp 174-177, 2008.
35. Z. Vizintin: Fractional Laser Technologies – Overview, 7th Croatian Congress of Plastic, Reconstructive and Aesthetic Surgery, Book of abstracts, Split, Croatia, 1-5 October, 2008.
36. J. Kozarev: Treatment of Stretch marks with fractional ablative Er:YAG laser, Belgrade, Serbia, June 2008.
37. C.Pidal: Estria Roja con Fractional Smooth ErYAG laser, VIII Curso Internacional de Procedimientos Estéticos Minimamente Invasivos "Avances en Medicina Estética y Cirugía Minimamente Invasiva", Lima, Peru, 2008.
38. K. Massoud: Fractional Laser Skin Resurfacing, International Aesthetic Laser Seminar, Dubai, October 2007.